

Scaling of Microtubule Force-Velocity Curves Obtained at Different Tubulin Concentrations

Marcel E. Janson* and Marileen Dogterom

FOM Institute AMOLF, Kruislaan 407, 1098 SJ Amsterdam, The Netherlands

(Received 5 June 2003; published 16 June 2004)

We present a single curve that describes the decay in average growth velocity for microtubules in response to a mechanical force. Curves obtained at two new and one previously studied tubulin concentrations coalesce when normalized with the growth velocity at zero load. This scaling provides direct evidence for a force-independent molecular off rate, in agreement with Brownian ratchet models. In addition, microtubule length changes were measured with a precision up to 10 nm, revealing that microtubules under load abruptly switch between different growth velocities.

DOI: 10.1103/PhysRevLett.92.248101

PACS numbers: 87.16.Ka, 82.35.Pq

Microtubules (MTs) are long and stiff biopolymers. They assemble from 8 nm long tubulin dimers that longitudinally bind to form protofilaments, and laterally connect to form a hollow tube of, on the average, 13 protofilaments [Fig. 1(a)] [1]. After assembly, one molecule of guanosine triphosphate (GTP) that is bound to the dimers is hydrolyzed to GDP. This hydrolysis destabilizes the MT structure, which enables MTs to switch occasionally to a state of rapid shrinkage, an event termed a catastrophe [1]. Filamentous protein aggregates like MTs and actin filaments can generate pushing forces when they polymerize close to cellular objects in living cells [2]. These forces play an important role in the internal organization of cells. For example, forces generated by MTs push the nucleus towards the cell middle in fission yeast [3] and are believed to be involved in the motion of chromosomes during mitosis [4].

Protein “polymerization motors” convert free energy derived from the assembly of proteins into mechanical work. In general, the force-velocity relation for a growing polymer buildup of N protofilaments can be written as $v(f) = \frac{\delta}{N}[k_{\text{on}}(f)C - k_{\text{off}}(f)]$, where δ is the length of the protein subunit, and $k_{\text{on}}C$ and k_{off} are the force-dependent molecular on and off rates for protein concentration C [5]. To understand the physical mechanisms of the polymerization motor and to establish how molecular on and off rates respond to force, quantitative data on single force-generating actin filaments or MTs are needed. In contrast to the amount of available theoretical work [6–9], experimental data are, however, still extremely rare [2]. Previously, we measured a force-velocity relation for single growing MTs for one set of conditions with a result that was suggestive of a force-independent off rate [10]. Direct proof for a force-independent off rate coming from experiments under a range of different conditions is, however, still lacking. Such proof would support a class of models based on a Brownian ratchet mechanism that have been put forward to describe both the MT and actin polymerization motor [7–9].

Here we present force-velocity data at two different tubulin concentrations that, combined with our previ-

ously published data, provide direct evidence for the fact that force reduces the molecular on rate without noticeably increasing the molecular off rate. We find that, on average, all available data can be mapped onto a single force-velocity relation by normalizing with the

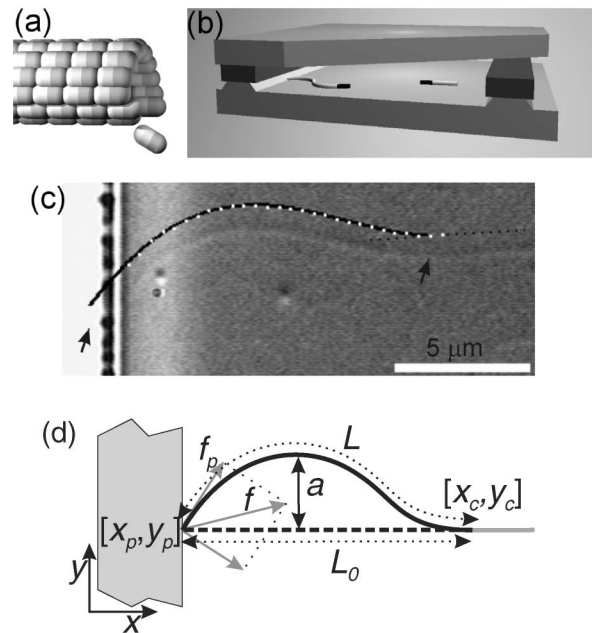


FIG. 1. (a) Lattice structure of tubulin dimers (white/gray) in a MT. (b) Schematic view of the experiments, not to scale. Randomly deposited seeds (black) nucleate MTs (white) in between barriers that are constructed on glass coverslips. (c) Example of a buckled MT. A fitted MT shape is plotted in black (shifted upwards). White dots indicate marker points used for fitting. The barrier contact point (left arrow, obscured by the barrier) and clamp position (right arrow) were found by optimizing all shape fits within one buckling event. The position of the clamp was forced to lie on a line intersecting the seed (dotted line). (d) Schematic sketch of an initially straight MT (dashed, length L_0) that buckles (L) and generates a parallel force f_p . MTs were unconstrained between their clamp position $[x_c, y_c]$ (gray) and the barrier-contact point $[x_p, y_p]$ where they can freely pivot.

growth velocity a zero load. This scaling behavior is expected if the off rate remains small compared to the on rate in the force regime that is studied. In addition, by improving our experimental and analysis methods, we were able to follow MT length changes under force at a resolution up to 10 nm. This allows us to show that changes in MT growth velocity previously observed for free growing MTs persist under force and that these changes occur abruptly, within 2 s.

To study force generation, MTs were grown from surface-attached nucleation sites, called seeds, and their buckling behavior was analyzed after the growing end contacted a rigid barrier [Figs. 1(b) and 1(c)]. The methods are identical to those described in [11] where, compared to earlier methods [10], we significantly improved the attachment of MT seeds. The force was varied by analyzing MTs nucleated at different distances L_0 from the barrier: a buckling MT nucleated by a strongly attached seed [Fig. 1(d)] generates a force $f_c \approx 20.19\kappa/L_0^2$ where κ is the flexural rigidity [10,12]. Force generation was studied at two different tubulin concentrations C_T [13]. The corresponding average growth velocities before buckling ($v_0 \pm$ standard error of the mean) were $1.88 \pm 0.03 \mu\text{m}/\text{min}$ ($C_T = 20 \mu\text{M}$) and $2.40 \pm 0.01 \mu\text{m}/\text{min}$ ($C_T = 28 \mu\text{M}$). At higher C_T values many MTs were created by self-nucleation causing problems in data analysis, while at lower values data acquisition was difficult because catastrophes often occurred before MTs reached the barriers [14]. The relation between catastrophe rate and growth velocity varies between different preparations of tubulin [11,14,15], explaining why in previous work, using more stable MTs, a force-velocity curve could be measured for $v_0 = 1.2 \mu\text{m}/\text{min}$ [10].

Buckling of the MTs was terminated either by a catastrophe or by sudden sliding of the MT end along the barrier [11]. The duration T of buckling events that were suitable for analysis (8 events at $20 \mu\text{M}$ and 21 at $28 \mu\text{M}$) was on average 59 s. Digitized microscopy images were analyzed every 2 s. For each time point, MT length and force were estimated by fitting the theoretical shape of a homogenous elastic rod to 29 marker points [Fig. 1(c)] [11]. The shape of an elastic rod and the forces acting on it are fully determined if the distance between the MT end points, the length of the MT, and two boundary conditions at the end points are known [12,16]. Strong seed binding allowed us to assume both the position and the angle of the seed with respect to the barrier to be fixed during buckling. The MT was assumed to pivot freely around its contact point with the barrier, and thus only the MT length remained to be fitted to determine the direction of the force and the force/rigidity ratio. This reduced number of fit parameters improved the length and force estimates compared to earlier methods, where three fit parameters were used [10]. To calibrate the forces, MT rigidities were measured by analyzing thermally induced deflections of the tips of freely growing MTs [17]. Surprisingly, the average κ was different for the different

values of C_T used, and the data were therefore calibrated depending on C_T : $\kappa = 21.2 \pm 1.7 \text{ pN } \mu\text{m}^2$ for $20 \mu\text{M}$ (23 MTs; the error is the standard error of the mean δ_κ) and $\kappa = 13.7 \pm 1.4 \text{ pN } \mu\text{m}^2$ for $28 \mu\text{M}$ (16 MTs).

An example of a fit result is given in Fig. 2(a), where both the length L and the force component along the direction of MT growth [f_p , Fig. 1(d)] are plotted before and during buckling. Figure 2(b) shows an enlargement of these data during buckling and Figs. 2(c) and 2(d) show two other examples of length data during buckling. Figures 2(b)–2(d) show that the length resolution σ_L on the data for force-generating MTs is much better than for freely growing MTs ($\sigma_{L,\text{free}} = 70 \text{ nm}$ [19]). This can be understood because upon initial buckling a small length increase ΔL is amplified to a much larger observable change in the amplitude of buckling $\Delta a = Z\Delta L$ [Fig. 1(d)]. For the geometry displayed the amplification factor Z is approximately equal to $0.62/\sqrt{\lambda}$, with λ the relative length increase since the initiation of buckling [20]. The resulting experimental length resolution was estimated by analyzing the observed variance in growth velocities as a function of λ [18]. The result of this analysis is shown in Fig. 2(e) and is used to determine the error bars in Figs. 2(b)–2(d). The resolution is initially very good ($\sigma_L < 12 \text{ nm}$ for $\lambda < 1\%$), but decreases when λ increases.

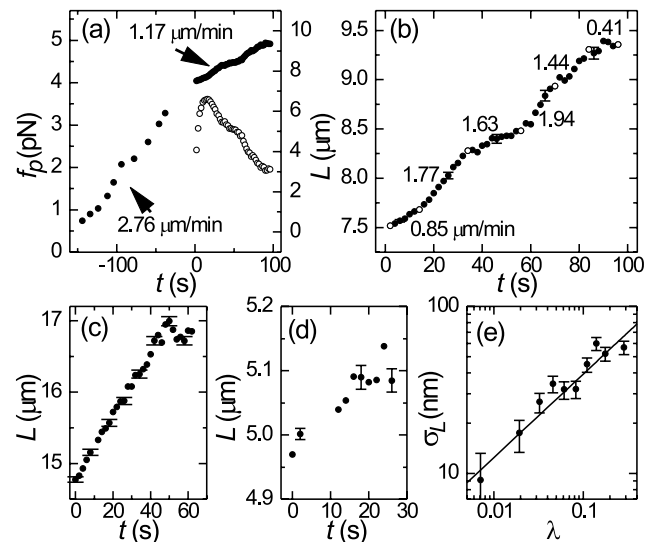


FIG. 2. (a) Fit results for f_p (left axis, open symbols) and L (right axis, closed symbols), for a MT at $C_T = 28 \mu\text{M}$. The average velocities before ($t < 0$) and during buckling ($t > 0$; v_T) are indicated. (b) Enlarged view on length data from Fig. 2(a). Open symbols demarcate periods with apparent constant velocity (indicated values). Error bars are derived from the fit shown in (e). (c),(d) Length data for two MTs ($C_T = 28 \mu\text{M}$) that experienced a catastrophe within 2 s of the last data point. $\langle f_p \rangle$ values are 0.7 and 10.6 pN, respectively. (e) σ_L as a function of λ . For 10 data points, $\sqrt{\frac{1}{2}\tau^2[\text{var}(v_{t=2\text{s}}) - \text{var}I]}$ is plotted together with the fitted result $\sigma_a\sqrt{\lambda}/0.62$ (straight line) [18].

The good length resolution allowed us to detect abrupt changes in growth velocity during buckling [see regions indicated in Fig. 2(b)]. Several observations suggest that free MTs can adopt different end structures as they grow [1,21–23], which may be correlated with observed changes in growth velocity [22]. Our data show that, under load, changes in assembly rate occur abruptly within 2 s [Fig. 2(b)] and that pause states often occur just before MTs switch to a catastrophe [Figs. 2(c) and 2(d)]. Five events that could be analyzed all the way to a catastrophe showed a similar pause of approximately 10 s, possibly reflecting an intermediate state between growth and rapid shrinkage [23,24].

In order to determine the response of *individual* MTs to force, we plotted in Fig. 3(a) for each buckling event the average force ($\langle f_p \rangle$) versus the average velocity ($v_T = [L(t=T) - L(t=0)]/T$ with error $\sqrt{\sigma_{L(t=T)}^2 + \sigma_{L(t=0)}^2}/T$).

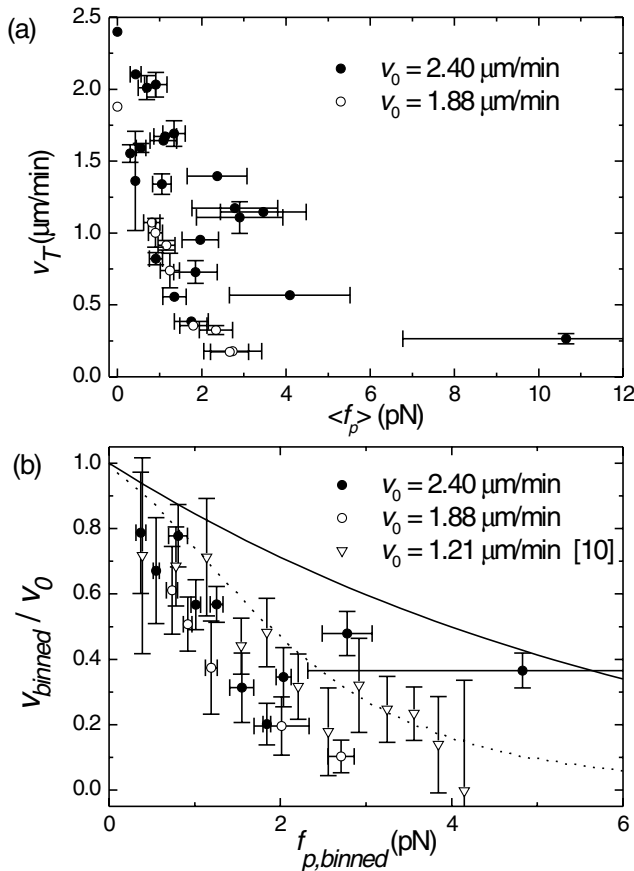


FIG. 3. (a) v_T and $\langle f_p \rangle$ values for individual buckling events at $C_T = 20 \mu\text{M}$ (open circles) and $28 \mu\text{M}$ (closed circles). v_0 is plotted at $\langle f_p \rangle = 0$. Error bars smaller than the symbol size are not plotted. (b) Average force-velocity curves obtained by binning 2 s segments with respect to f_p . Data are normalized with v_0 and compared with previous data (triangles) [10]. The standard error in the binned velocities and the standard deviation in the binned forces are plotted. The theoretical curve (see text) is a simulation result for $C_T = 20 \mu\text{M}$ and the measured k_{on} and k_{off} , but hardly differs for the other two conditions in the plotted range.

The error plotted for $\langle f_p \rangle$ consists of three approximately equal parts: (1) $\langle f_p \rangle \delta \kappa / \kappa$ is the error due to a limited accuracy on κ . (2) The standard deviation of the averaged f_p values accounts for the force not being strictly constant during buckling [in Fig. 2(a), f_p slowly decreases as the MT grows 25% relative to its initial length; the relative length increases, and the consequent drop in f_p was less for all other buckling events (average 8%)]. (3) Errors in the determination of the clamp position and barrier contact point [e.g., Fig. 1(c)] were estimated by feeding simulated data to the fitting algorithm. Figure 3(a) shows that for both values of C_T there is a clear downward trend of v_T with $\langle f_p \rangle$. For a given force, the vertical scatter is, however, larger than the error bars on the velocity. This is to be expected given the intrinsic variability in growth velocities that was seen in Fig. 2.

To establish the *average* response of the velocity to force under different growth conditions, data on all MTs were combined. For each concentration, the measured instantaneous velocities over 2 s segments ($v_{T=2 \text{ s}}$; $N = 608$ for $C_T = 28 \mu\text{M}$ and $N = 211$ for $C_T = 20 \mu\text{M}$) were sorted and binned with respect to the average force during that segment (number of segments per bin is 60 at $28 \mu\text{M}$ and 40 at $20 \mu\text{M}$). The average velocities calculated in each bin were normalized with v_0 (2.40 or $1.88 \mu\text{m}/\text{min}$) and, together with the results from earlier work ($v_0 = 1.2 \mu\text{m}/\text{min}$) [10], plotted in Fig. 3(b). Even though there is scatter in the data, the normalized force-velocity curves do not show any v_0 -dependent trend and appear to coalesce onto one curve.

Given the general force-velocity relation given in the introduction, we can write the normalized velocity under load in the following way: $v(f_p)/v_0 = \frac{\delta}{N} [k_{\text{on}}(f_p)C_T - k_{\text{off}}(f_p)] / \frac{\delta}{N} [k_{\text{on}}(0)C_T - k_{\text{off}}(0)]$. By analyzing v_0 as a function of C_T for our tubulin preparation (data not shown) [15], we estimated for free MT growth $k_{\text{on}}(0) = 2.65 \pm 0.27 \text{ s}^{-1} \mu\text{M}^{-1}$ and $k_{\text{off}}(0) = 5.6 \pm 2.9 \text{ s}^{-1}$, which are both values that fall within the range of published data [1]. For the C_T values studied (20 and $28 \mu\text{M}$) we may thus neglect $k_{\text{off}}(0)$ relative to $k_{\text{on}}(0)C_T$ in the denominator. If the decrease in growth velocity under load is solely caused by a decreased on rate and not by an increased off rate, we may also neglect k_{off} for small and moderate forces in the numerator yielding $v(f_p)/v(0) \approx k_{\text{on}}(f_p)/k_{\text{on}}(0)$. A constant k_{off} should thus give a normalized velocity that is independent of C_T and v_0 , just as is observed. The observed scaling also suggests that GTP hydrolysis, which causes MTs to undergo catastrophes, has no influence on the force-velocity behavior, at least not in the force regime studied here. At any given force, catastrophes occur at different time scales for the three conditions studied [11], but the normalized velocity appears unaffected by this. Vice versa, the earlier reported force dependency of catastrophes seems only a result of the reduction in growth velocity, which can also be explained by assuming a constant k_{off} [11].

The now converging evidence for a force-independent k_{off} supports models that describe a force-generating MT as a Brownian ratchet. In this mechanistic view only k_{on} is affected by force, in a way that depends on the assumed geometrical details at the growing MT end [7]. In fact, changes in these details during growth, and corresponding different responses to force, may very well contribute to the variability in growth velocity we observe under load. On average, the experimentally obtained force-velocity relation seems to be well approximated by a specific Brownian ratchet model that was introduced by Mogilner and Oster for MTs and simulated for a finite off rate by v. Doorn *et al.* [9] [Fig. 3(b), dotted line]. In this model, protofilaments are assumed to grow independently of each other, leading to an irregularly shaped MT end.

In conclusion, we have shown that all available MT force-velocity data can be mapped onto a single curve for the normalized average velocity. This establishes that force primarily changes the rate of subunit addition, and that protein disassembly events from the MT are force independent. We have in addition shown that length changes of MTs under load can be followed with high resolution, revealing that velocity fluctuations observed for free MTs persist under load. In the future, data on MT growth near the stall force, which are inherently difficult to obtain with the current method, will hopefully become available from experiments with optical tweezers [25]. In addition, with the intrinsic response of MT dynamics to force now well established, one of our next goals will be to investigate whether regulatory proteins that interact with the ends of growing MTs *in vivo* [26] are able to change the molecular growth details and thereby the force-velocity behavior.

We are grateful to Cătălin Tănase, Bela Mulder, Jacob Kerssemakers, and Harm Geert Muller for helpful discussions and a critical reading of the manuscript. This work is part of the research program of the “Stichting voor Fundamenteel Onderzoek der Materie (FOM),” which is financially supported by the “Nederlandse organisatie voor Wetenschappelijk Onderzoek (NWO).”

*Present address: University of Pennsylvania, Department of Cell and Developmental Biology, 421 Curie Blvd., Philadelphia, PA 19104-6058, USA.

- [1] A. Desai and T.J. Mitchison, *Annu. Rev. Cell Dev. Biol.* **13**, 83 (1997).
- [2] J.A. Theriot, *Traffic* **1**, 19 (2000); A. Mogilner and G. Oster, *Curr. Biol.* **13**, R721 (2003).
- [3] P.T. Tran *et al.*, *J. Cell Biol.* **153**, 397 (2001).
- [4] A. Khodjakov, I.S. Gabashvili, and C.L. Rieder, *Cell Motil. Cytoskeleton* **43**, 179 (1999); S. Inoue and E.D. Salmon, *Mol. Biol. Cell* **6**, 1619 (1995).
- [5] H. A. Kramers, *Physica (Amsterdam)* **7**, 284 (1940); T.L. Hill, *Linear Aggregation Theory in Cell Biology* (Springer-Verlag, New York, 1987).
- [6] A. B. Kolomeisky and M. E. Fisher, *Biophys. J.* **80**, 149 (2001); A. E. Carlsson, *Phys. Rev. E* **62**, 7082 (2000).
- [7] M. Dogterom *et al.*, *Appl. Phys. A* **75**, 331 (2002).
- [8] C. S. Peskin, G. M. Odell, and G. F. Oster, *Biophys. J.* **65**, 316 (1993).
- [9] A. Mogilner and G. Oster, *Eur. Biophys. J. Biophys. Lett.* **28**, 235 (1999); G. S. v. Doorn, C. Tanase, B. M. Mulder, and M. Dogterom, *Eur. Biophys. J. Biophys. Lett.* **29**, 2 (2000).
- [10] M. Dogterom and B. Yürke, *Science* **278**, 856 (1997).
- [11] M. E. Janson, M. E. de Dood, and M. Dogterom, *J. Cell Biol.* **161**, 1029 (2003).
- [12] F. Gittes, E. Meyhofer, S. Baek, and J. Howard, *Biophys. J.* **70**, 418 (1996).
- [13] Sample conditions: MRB80 buffer (80 mM K-PIPES, 1 mM EGTA, 4 mM MgCl₂, pH 6.8) plus 1 mM GTP and 10 mg/ml BSA. An oxygen scavenging system [10] was used at $C_T = 20 \mu\text{M}$. The growth of MT plus ends was observed with DIC microscopy at 23 °C (Leica DMIRB inverted microscope; 100× oil immersion objective, numerical aperture 1.3).
- [14] D. K. Fygenson, E. Braun, and A. Libchaber, *Phys. Rev. E* **50**, 1579 (1994).
- [15] R. A. Walker *et al.*, *J. Cell Biol.* **107**, 1437 (1988).
- [16] L. D. Landau and E. M. Lifshitz, *Theory of Elasticity* (Pergamon, New York, 1986).
- [17] L. Cassimeris, D. Gard, P.T. Tran, and H. P. Erickson, *J. Cell Sci.* **114**, 3025 (2001).
- [18] Differences between the measured instantaneous ($\tau = 2$ s) and average velocity under load (v_T) are caused by intrinsic variability in growth velocity and the limited length resolution: $\text{var}(v_\tau - v_T) = \text{var}_I + \text{var}_L$. During $\tau = 2$ s, λ , and Z remain nearly constant, and we may write $\text{var}_L = 2\sigma_L^2/\tau^2 = 2\sigma_a^2/Z^2\tau^2 \propto \lambda$. Here, σ_a is the error in a . All 29 analyzed buckling events were subdivided into 2 s segments for which $v_{\tau=2\text{ s}}$ and λ were calculated. The resulting 819 data points were sorted and binned (10 bins) with respect to λ . For each bin the variance plus its error was calculated and the equation for $\text{var}(v_\tau - v_T)$ was fitted with the following result: $\text{var}_I = 0.24 \pm 0.10 \mu\text{m}^2 \text{min}^{-2}$ and $\sigma_a = 77 \pm 5$ nm.
- [19] Obtained from repeated length measurements on a freely growing MT.
- [20] This equation was obtained by analysis of calculated buckling curves.
- [21] R. F. Gildersleeve *et al.*, *J. Biol. Chem.* **267**, 7995 (1992); D. Chretien and S. D. Fuller, *J. Mol. Biol.* **298**, 663 (2000).
- [22] D. Chretien, S. D. Fuller, and E. Karsenti, *J. Cell Biol.* **129**, 1311 (1995).
- [23] I. Arnal, E. Karsenti, and A. A. Hyman, *J. Cell Biol.* **149**, 767 (2000).
- [24] P.T. Tran, R. A. Walker, and E. D. Salmon, *J. Cell Biol.* **138**, 105 (1997); I.M. Janosi, D. Chretien, and H. Flyvbjerg, *Biophys. J.* **83**, 1317 (2002).
- [25] J.W.J. Kerssemakers, M. E. Janson, A. Van der Horst, and M. Dogterom, *Appl. Phys. Lett.* **83**, 4441 (2003); H.T. Schek and A. J. Hunt, *Biophys. J. Suppl.* **84**, 113A (2003).
- [26] J. Howard and A. A. Hyman, *Nature (London)* **422**, 753 (2003).